

Title: The Radius of Neutron Stars and the Dense Matter Equation of State

Date: Feb 06, 2014 01:00 PM

URL: <http://pirsa.org/14020087>

Abstract: The equation of state of matter at and above nuclear densities remains a major theoretically uncertain prediction of QCD. Observations of the mass-radius relationship of neutron stars constrain, and can directly measure, the dense matter equation of state. I will discuss how measurements of neutron star radii have already constrained the dEOS, and how future work will directly measure the dEOS, providing an important constraint on models of the strong force.

The Radius of Neutron Stars



Bob Rutledge
McGill University

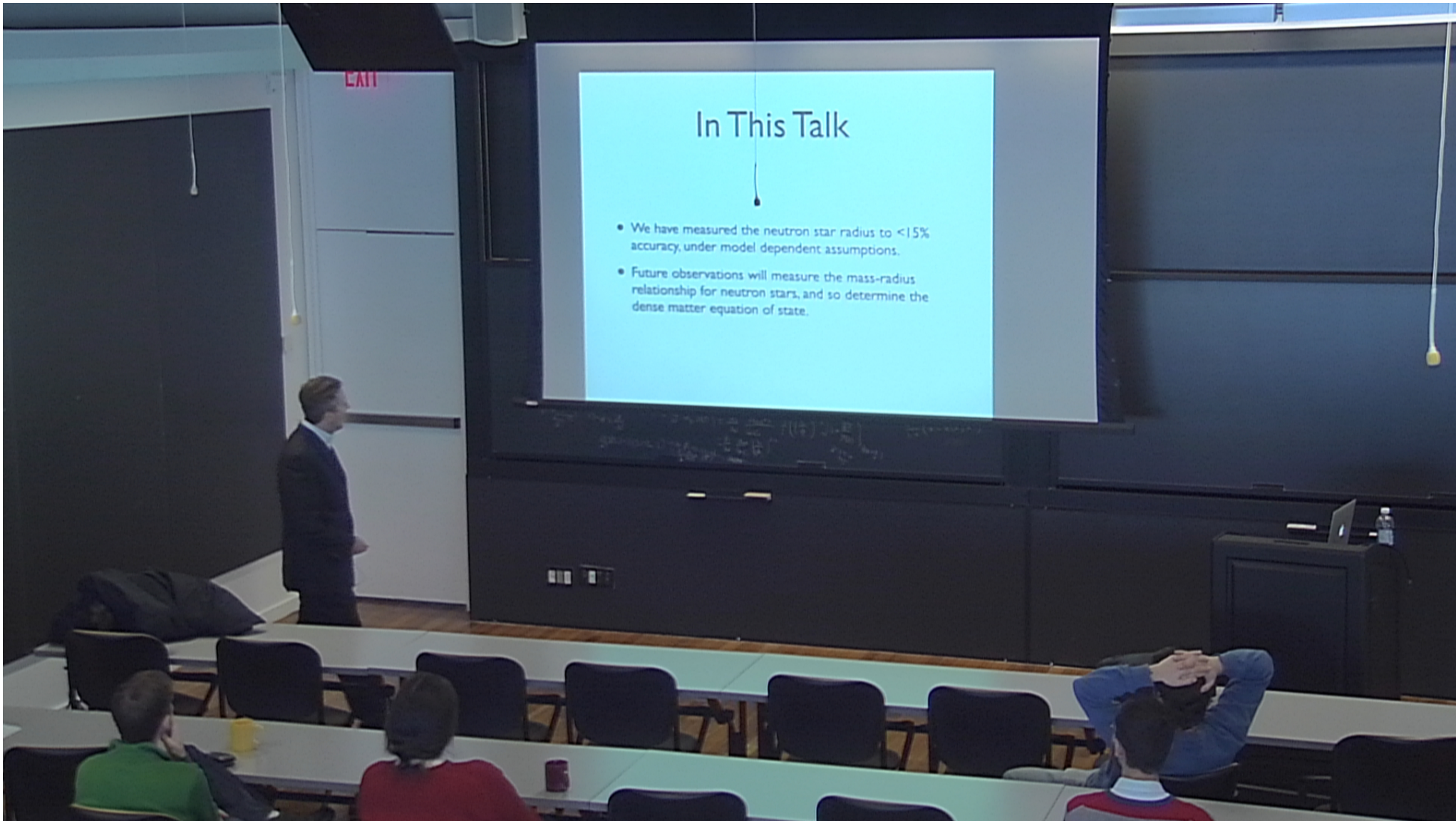
Collaborators: **Sebastien Guillot (McGill)**, Mathieu Servillat (Saclay) Natalie Webb (Toulouse), Ed Brown (MSU) Lars Bildsten (UCSB/KITP) George Pavlov (PSU) Vyacheslav Zavlin (MSFC).

In This Talk

- We have measured the neutron star radius to $<15\%$ accuracy, under model dependent assumptions.
- Future observations will measure the mass-radius relationship for neutron stars, and so determine the dense matter equation of state.

In This Talk

- We have measured the neutron star radius to $<15\%$ accuracy, under model dependent assumptions.
- Future observations will measure the mass-radius relationship for neutron stars, and so determine the dense matter equation of state.



Solving Quantum Chromodynamics At Finite Density - Neutron Stars are Unique Astrophysical Laboratories

- 1932: Since discovery of neutron (Chadwick 1932), how the strong force works to mediate attraction between protons and neutrons has been a major question for physics.
- 1930s-1960s: Strong force is a non-superpositional force, multi-body in nature -- parameterization with Skyrme potential had (limited) success explaining the properties of small nuclei.
- 1960s: Discovery of quarks, and development of QCD explained the formation of neutrons, protons, mesons, hyperons.... This is QCD at finite energy (temperature, QCDt). It does an outstanding job of explaining the existence of these particles, and their one-to-one interactions. But we have no exact theoretical apparatus to perform the many-body interaction calculations. Thus we rely on approximate methods of effective-field-theories (Brueckner-Betha-Goldstone Theory, Green's function theory, and relativistic mean-field theory).
- Today: QCD is not an exact theory at finite density (QCDd). Where this becomes relevant is above nuclear density ($>2.35 \times 10^{14} \text{ g cm}^{-3}$), and for asymmetric matter (many more neutrons than protons).
- It is technically impossible to create cold nuclear matter above nuclear density in terrestrial laboratories. However, in the cores of neutron stars, gravitational force compresses matter to supernuclear densities.
- Thus: Neutron Stars are unique sites of cold QCDd in the universe, precisely as black holes are the unique sites for strong field gravity.
- **If we want to solve QCDd, neutron stars will be the astrophysical tool for solving it.**

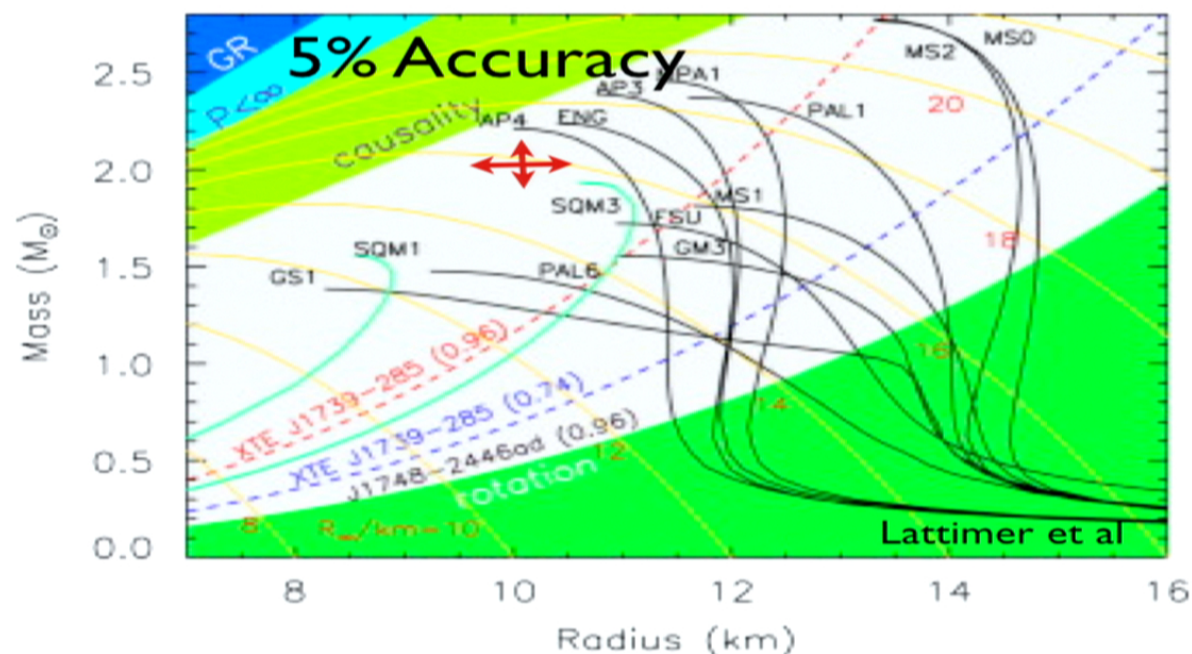
The Dense Matter Equation of State is an important Strong Force Regime

Each different proposed dEOS produces a different mass-radius relationship for neutron stars.

Thus, measure the mass-radius relationship of neutron stars, and you have a measurement of the dEOS.

Precision requirement -- 5% in mass and radius, separately.

A larger uncertainty is useless to nuclear physics.



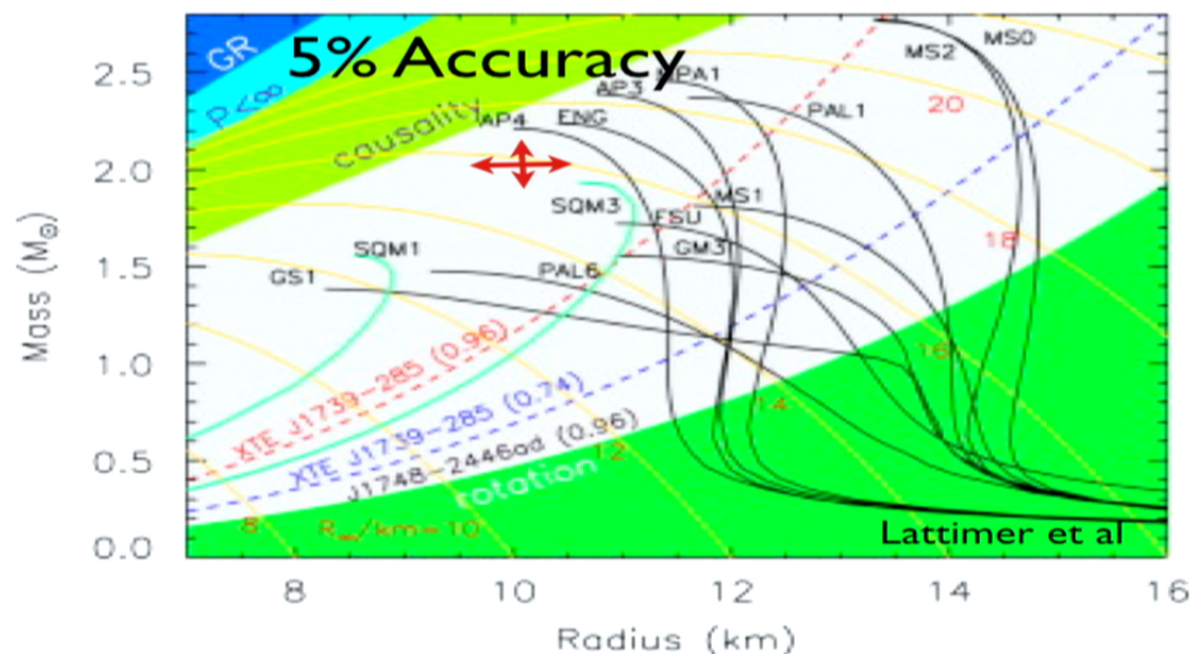
The Dense Matter Equation of State is an important Strong Force Regime

Each different proposed dEOS produces a different mass-radius relationship for neutron stars.

Thus, measure the mass-radius relationship of neutron stars, and you have a measurement of the dEOS.

Precision requirement -- 5% in mass and radius, separately.

A larger uncertainty is useless to nuclear physics.



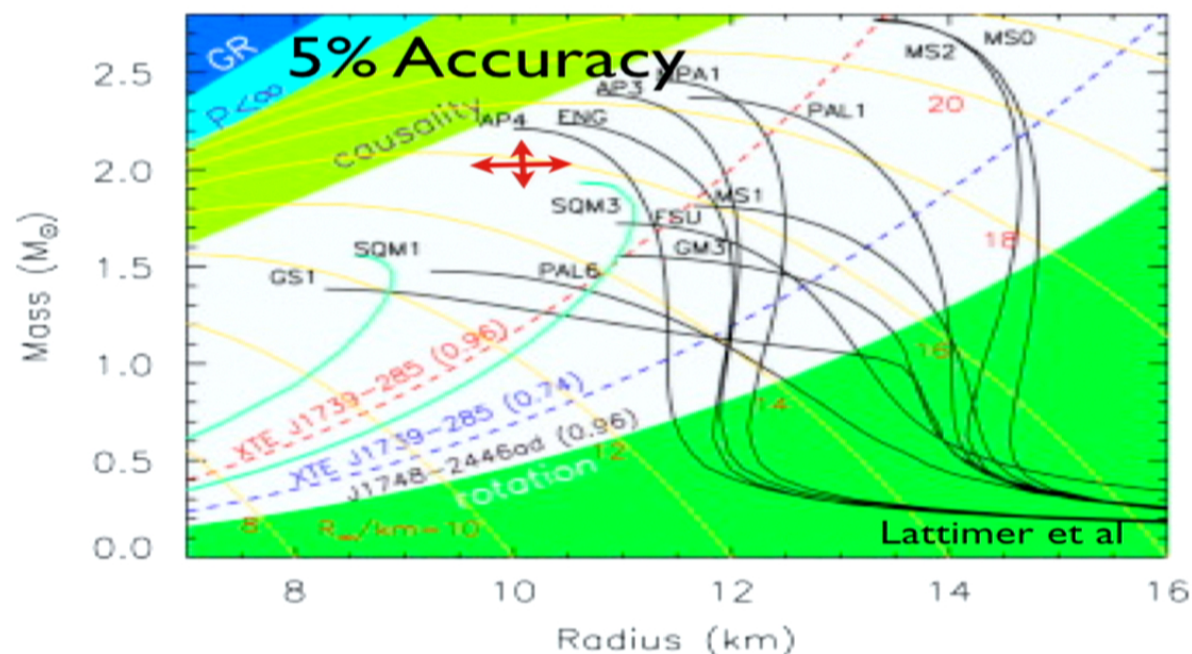
The Dense Matter Equation of State is an important Strong Force Regime

Each different proposed dEOS produces a different mass-radius relationship for neutron stars.

Thus, measure the mass-radius relationship of neutron stars, and you have a measurement of the dEOS.

Precision requirement -- 5% in mass and radius, separately.

A larger uncertainty is useless to nuclear physics.



Timing measurements -- which permit NS mass measurements -- are limited in precision by the stability of rotation in NS (very high) and the precision of the comparison clocks (very high).

VERY LOW SYSTEMATIC UNCERTAINTIES

Result: Masses are measured to 0.0001%



Timing measurements -- which permit NS mass measurements -- are limited in precision by the stability of rotation in NS (very high) and the precision of the comparison clocks (very high).

VERY LOW SYSTEMATIC UNCERTAINTIES

Result: Masses are measured to 0.0001%

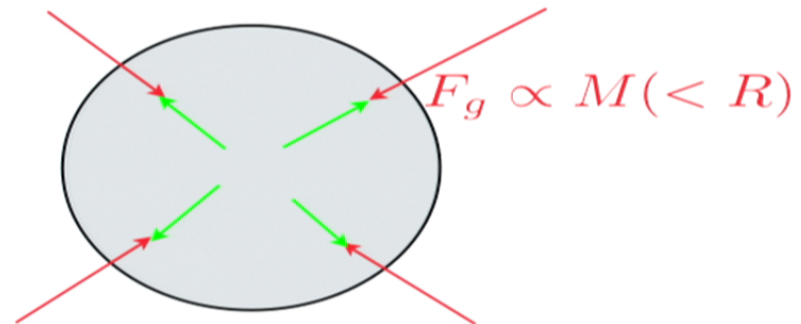


From Neutron Star Mass-Radius Relation to the Equation of State

$$P = f(\rho)$$

- Lindblom (1992) showed that each Dense Matter Equation of State maps to a unique Mass-Radius relationship for neutron stars.
- Ozel and Psaltis (2009) demonstrate how to perform the inverse problem: take the mass-radius relationship, and produce an equation of state. Only ~5-7 such objects are needed, but “with different masses”, to derive a new dense matter equation of state.
- Thus, measurement of the neutron star mass-radius relationship would implicate a unique dEOS.

Short Course:
Gravity pulls inward
Pressure Pushes Outward
Result: $R=f(M)$



Timing measurements -- which permit NS mass measurements -- are limited in precision by the stability of rotation in NS (very high) and the precision of the comparison clocks (very high).

VERY LOW SYSTEMATIC UNCERTAINTIES

Result: Masses are measured to 0.0001%



Timing measurements -- which permit NS mass measurements -- are limited in precision by the stability of rotation in NS (very high) and the precision of the comparison clocks (very high).

VERY LOW SYSTEMATIC UNCERTAINTIES

Result: Masses are measured to 0.0001%



Timing measurements -- which permit NS mass measurements -- are limited in precision by the stability of rotation in NS (very high) and the precision of the comparison clocks (very high).

VERY LOW SYSTEMATIC UNCERTAINTIES

Result: Masses are measured to 0.0001%



Timing measurements -- which permit NS mass measurements -- are limited in precision by the stability of rotation in NS (very high) and the precision of the comparison clocks (very high).

VERY LOW SYSTEMATIC UNCERTAINTIES

Result: Masses are measured to 0.0001%



Timing measurements -- which permit NS mass measurements -- are limited in precision by the stability of rotation in NS (very high) and the precision of the comparison clocks (very high).

VERY LOW SYSTEMATIC UNCERTAINTIES

Result: Masses are measured to 0.0001%





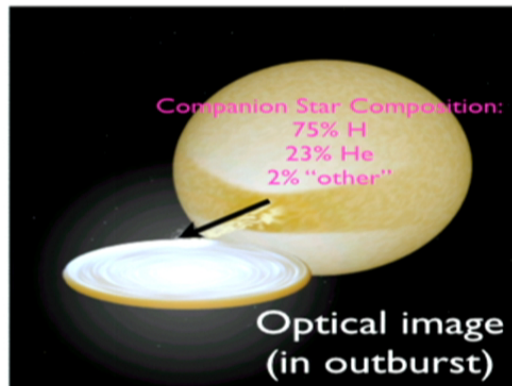
Quiescent Low Mass X-ray Binaries



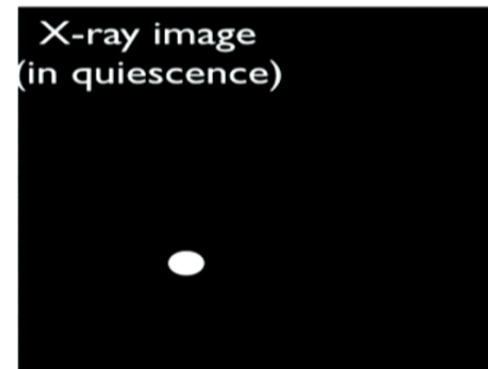
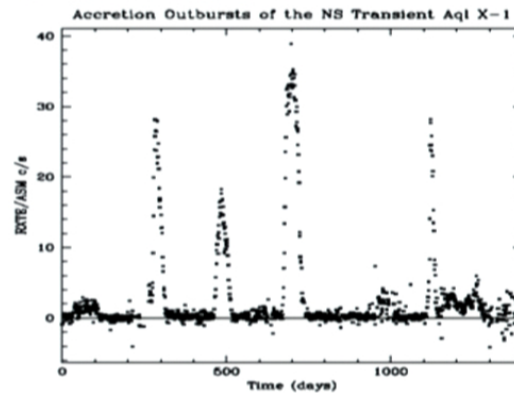
Quiescent Low Mass X-ray Binaries



Quiescent Low Mass X-ray Binaries (qLMXB)



Outburst



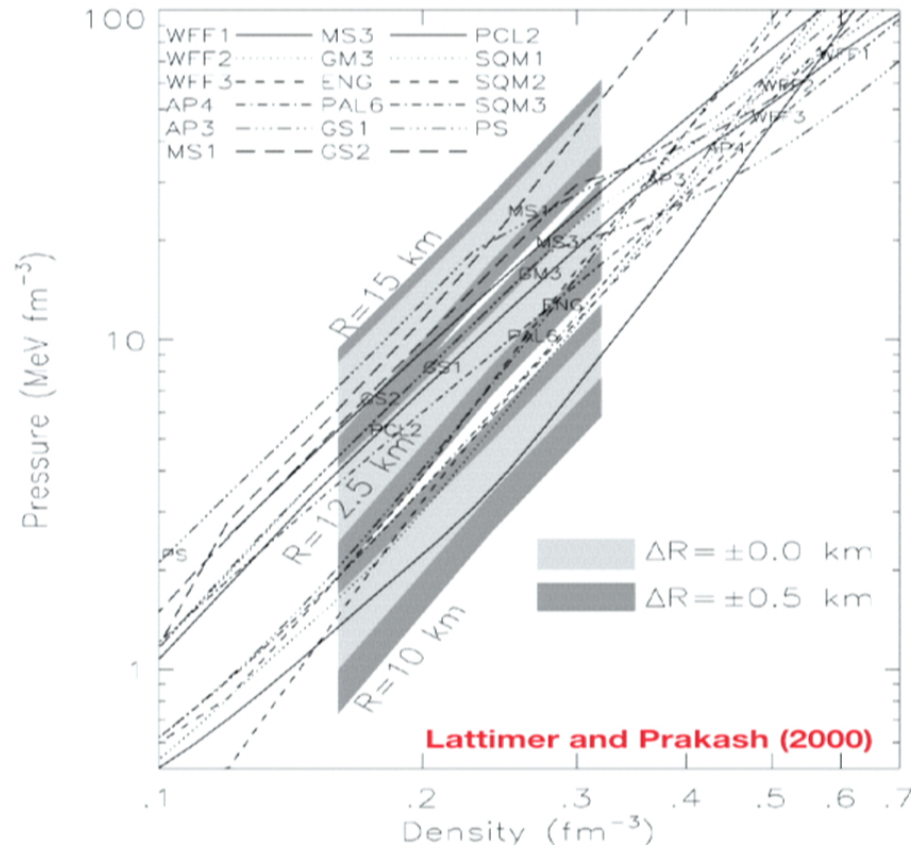
Quiescence

- Transient LMXBs in quiescence are H atmosphere neutron stars, powered by a core heated through equilibrium nuclear reactions in the crust.

Brown, Bildsten & RR (1998)

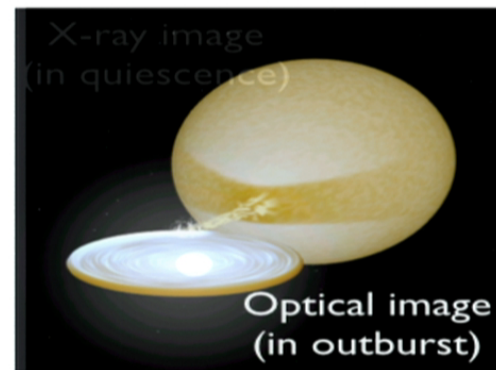
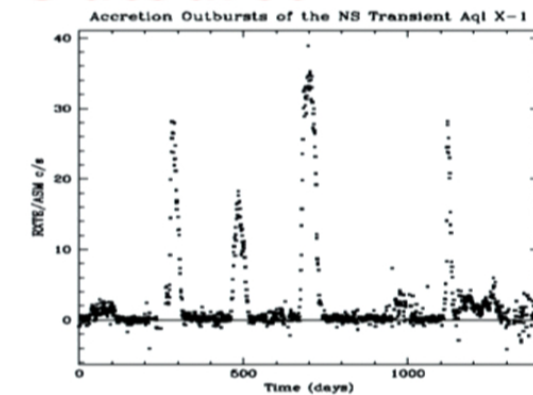
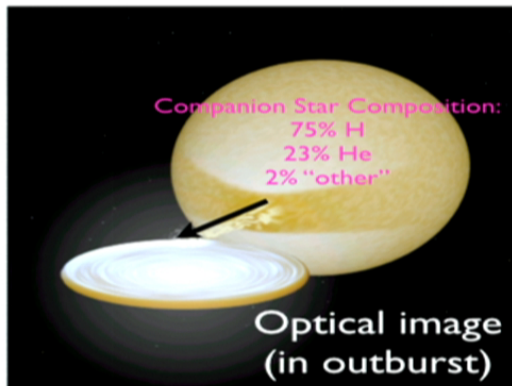
Estimated Equations of State

- Different calculational (approximation) methods
- Different input physics
- Different nuclear parameters (example: nuclear compressibility as a function of fractional neutron excess).



Quiescent Low Mass X-ray Binaries (qLMXB)

Outburst

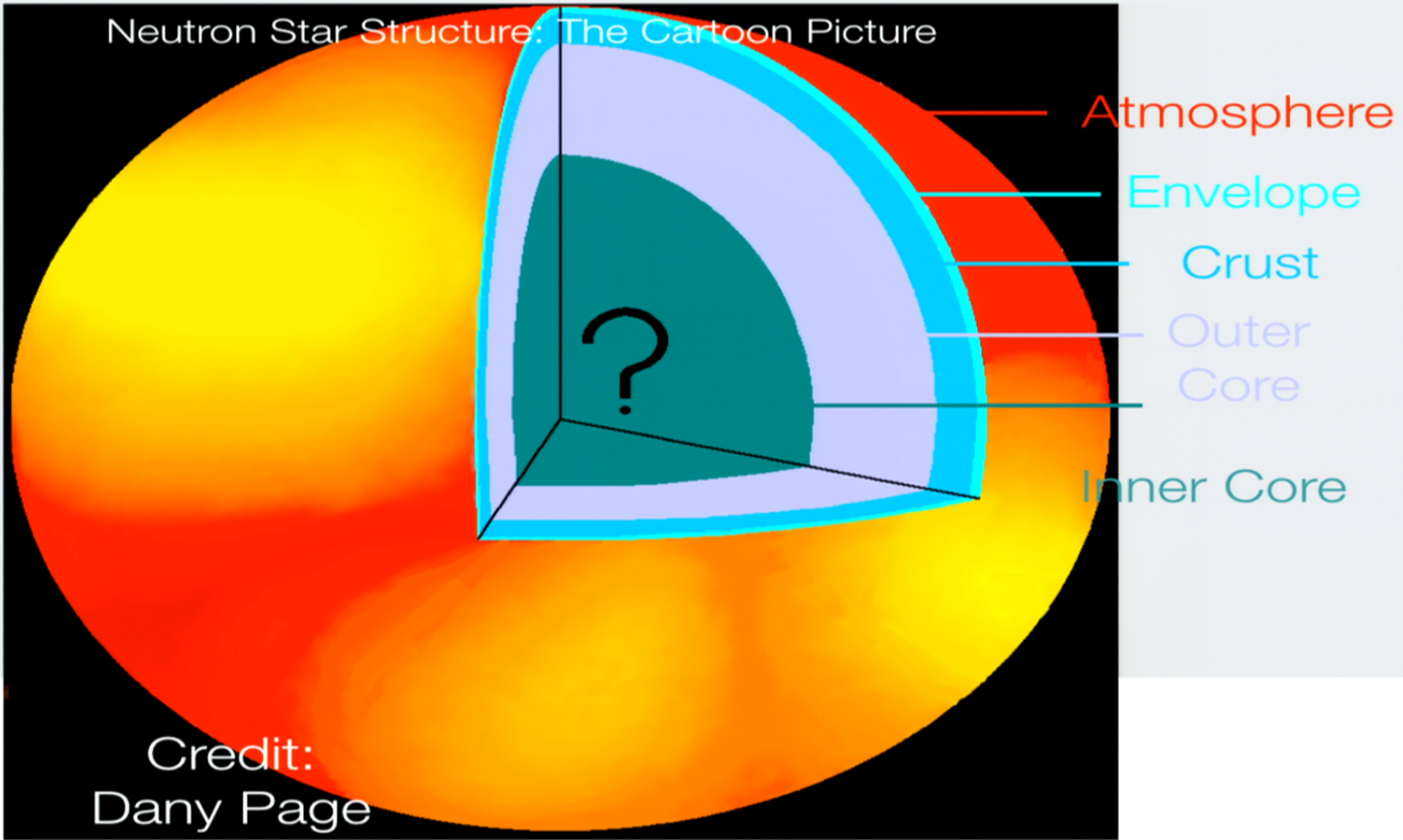


Quiescence

- Transient LMXBs in quiescence are H atmosphere neutron stars, powered by a core heated through equilibrium nuclear reactions in the crust.

Brown, Bildsten & RR (1998)

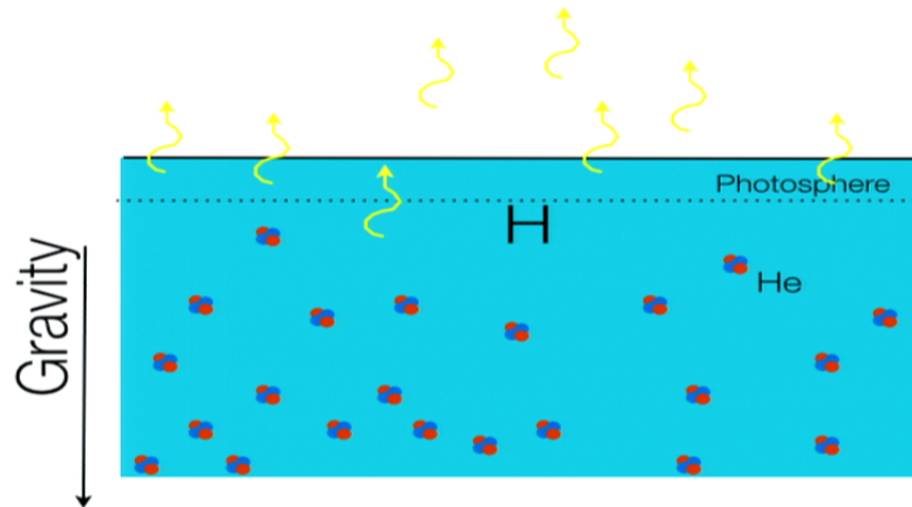
Neutron Star Structure: The Cartoon Picture



Credit:
Dany Page

qLMXBs, in this scenario, have pure Hydrogen atmospheres

- When accretion stops, the He (and heavier elements, gravitationally settle on a timescale of ~ 10 s of seconds (like rocks in water), leaving the photosphere to be pure Hydrogen (Alcock & Illarionov 1980, Bildsten et al 1992).



Brown, Bildsten & RR (1998)

Emergent Spectrum of a Neutron Star Hydrogen Atmosphere

• H atmosphere calculated Spectra are ab initio radiative transfer calculations using the Eddington equations.

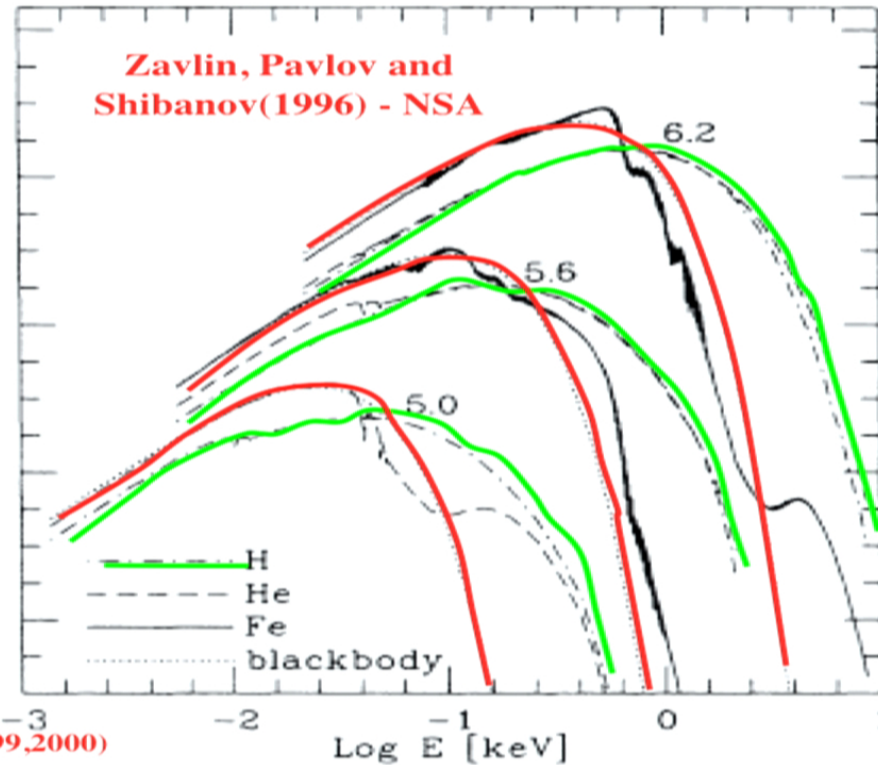
• Rajagopal and Romani (1996); Zavlin et al (1996); Pons et al (2002; Heinke et al (2006) -- NSATMOS; Gaensicke, Braje & Romani (2001); Haakonsen et al (2012)

All comparisons show consistency within ~few % (e.g. Webb et al 2007, Haakonsen 2012).

“Vetted”: X-ray spectra of Zavlin, Heinke together have been used in several dozen works.

$$F = 4\pi T_{eff,\infty}^4 \left(\frac{R_\infty}{D} \right)^2$$

$$R_\infty = \frac{R}{\sqrt{1 - \frac{2GM}{c^2 R}}}$$



Emergent Spectrum of a Neutron Star Hydrogen Atmosphere

• H atmosphere calculated Spectra are ab initio radiative transfer calculations using the Eddington equations.

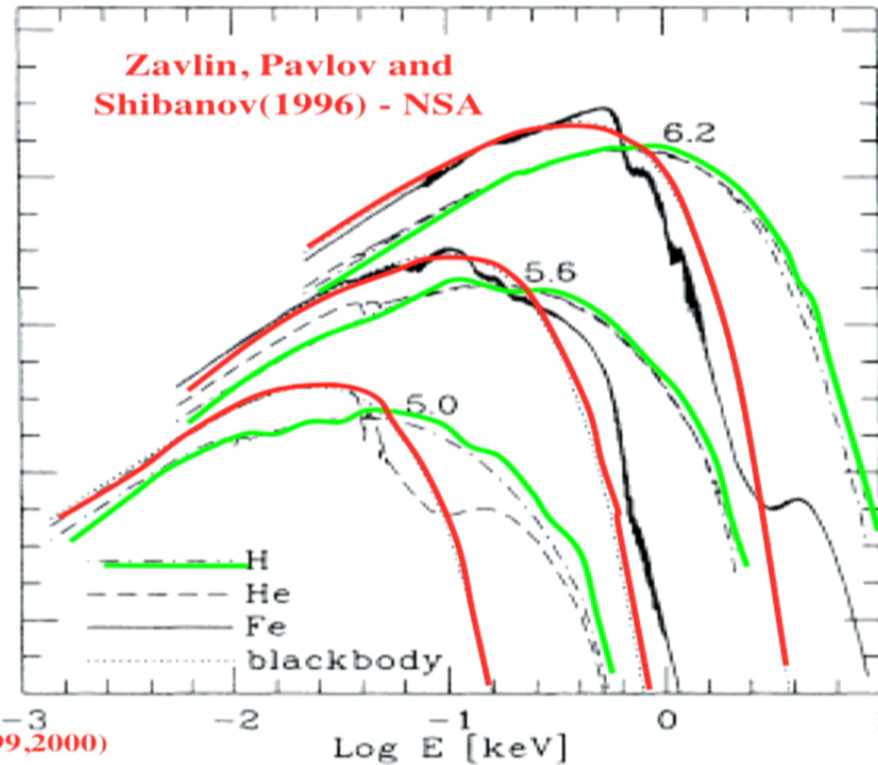
• Rajagopal and Romani (1996); Zavlin et al (1996); Pons et al (2002; Heinke et al (2006) -- NSATMOS; Gaensicke, Braje & Romani (2001); Haakonsen et al (2012)

All comparisons show consistency within ~few % (e.g. Webb et al 2007, Haakonsen 2012).

“Vetted”: X-ray spectra of Zavlin, Heinke together have been used in several dozen works.

$$F = 4\pi T_{eff,\infty}^4 \left(\frac{R_\infty}{D} \right)^2$$

$$R_\infty = \frac{R}{\sqrt{1 - \frac{2GM}{c^2 R}}}$$



Non-Equilibrium Processes in the Outer Crust
Beginning with ^{56}Fe (Haensel & Zdunik 1990, 2003)

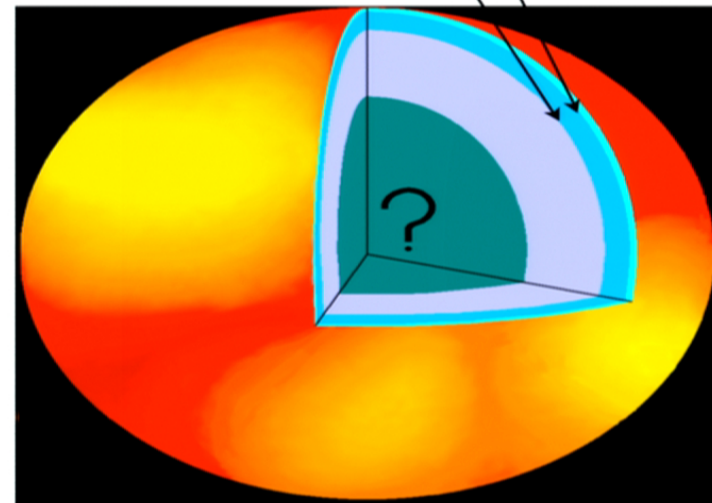
ρ (g cm^{-3})	Reaction	$\Delta\rho/\rho$	Q (Mev/np)
$1.5 \cdot 10^9$	$^{56}\text{Fe} \Rightarrow ^{56}\text{Cr} - 2e^- + 2\nu_e$	0.08	0.01
$1.1 \cdot 10^{10}$	$^{56}\text{Cr} \Rightarrow ^{56}\text{Ti} - 2e^- + 2\nu_e$	0.09	0.01
$7.8 \cdot 10^{10}$	$^{56}\text{Ti} \Rightarrow ^{56}\text{Ca} - 2e^- + 2\nu_e$	0.1	0.01
$2.5 \cdot 10^{10}$	$^{56}\text{Ca} \Rightarrow ^{56}\text{Ar} - 2e^- + 2\nu_e$	0.11	0.01
$3.1 \cdot 10^{10}$	$^{56}\text{Ar} \Rightarrow ^{52}\text{S} + 4n - 2e^- + 2\nu_e$	0.12	0.01

Non-Equilibrium Processes in the Inner Crust

ρ (g cm^{-3})	Reaction	X_n	Q (Mev/np)
$9.1 \cdot 10^{11}$	$^{52}\text{S} \Rightarrow ^{46}\text{Si} + 6n - 2e^- + 2\nu_e$	0.07	0.09
$1.1 \cdot 10^{12}$	$^{46}\text{Si} \Rightarrow ^{40}\text{Mg} + 6n - 2e^- + 2\nu_e$	0.07	0.09
$1.5 \cdot 10^{12}$	$^{40}\text{Mg} \Rightarrow ^{34}\text{Ne} + 6n - 2e^- + 2\nu_e$		
	$^{34}\text{Ne} + ^{34}\text{Ne} \Rightarrow ^{68}\text{Ca}$	0.29	0.47
$1.8 \cdot 10^{12}$	$^{68}\text{Ca} \Rightarrow ^{62}\text{Ar} + 6n - 2e^- + 2\nu_e$	0.39	0.05
$2.1 \cdot 10^{12}$	$^{62}\text{Ar} \Rightarrow ^{56}\text{S} + 6n - 2e^- + 2\nu_e$	0.45	0.05
$2.6 \cdot 10^{12}$	$^{56}\text{S} \Rightarrow ^{50}\text{Si} + 6n - 2e^- + 2\nu_e$	0.5	0.06
$3.3 \cdot 10^{12}$	$^{50}\text{Si} \Rightarrow ^{44}\text{Mg} + 6n - 2e^- + 2\nu_e$	0.55	0.07
$4.4 \cdot 10^{12}$	$^{44}\text{Mg} \Rightarrow ^{36}\text{Ne} + 6n - 2e^- + 2\nu_e$		
	$^{36}\text{Ne} + ^{36}\text{Ne} \Rightarrow ^{72}\text{Ca}$		
$5.8 \cdot 10^{12}$	$^{68}\text{Ca} \Rightarrow ^{62}\text{Ar} + 6n - 2e^- + 2\nu_e$	0.61	0.28
$7.0 \cdot 10^{12}$	$^{62}\text{Ar} \Rightarrow ^{60}\text{S} + 6n - 2e^- + 2\nu_e$	0.7	0.02
$9.0 \cdot 10^{12}$	$^{60}\text{S} \Rightarrow ^{54}\text{Si} + 6n - 2e^- + 2\nu_e$	0.73	0.02
$1.1 \cdot 10^{13}$	$^{54}\text{Si} \Rightarrow ^{48}\text{Mg} + 6n - 2e^- + 2\nu_e$	0.76	0.03
$1.1 \cdot 10^{13}$	$^{48}\text{Mg} + ^{48}\text{Mg} \Rightarrow ^{96}\text{Cr}$	0.79	0.41
$1.1 \cdot 10^{13}$	$^{96}\text{Cr} \Rightarrow ^{88}\text{Ti} + 8n - 2e^- + 2\nu_e$	0.8	0.01

Deep Crustal Heating

Begins Here
 Ends Here



1.47 Mev per np

Brown, Bildsten & RR (1998)

Non-Equilibrium Processes in the Outer Crust
Beginning with ^{56}Fe (Haensel & Zdunik 1990, 2003)

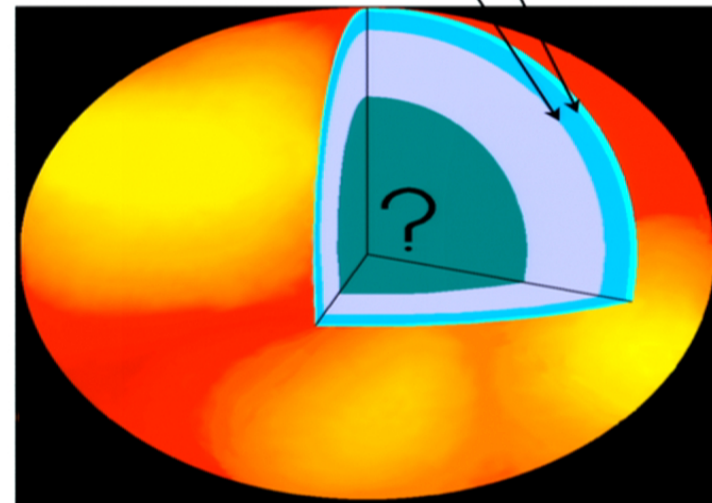
ρ (g cm^{-3})	Reaction	$\Delta\rho/\rho$	Q (Mev/np)
$1.5 \cdot 10^9$	$^{56}\text{Fe} \Rightarrow ^{56}\text{Cr} - 2e^- + 2\nu_e$	0.08	0.01
$1.1 \cdot 10^{10}$	$^{56}\text{Cr} \Rightarrow ^{56}\text{Ti} - 2e^- + 2\nu_e$	0.09	0.01
$7.8 \cdot 10^{10}$	$^{56}\text{Ti} \Rightarrow ^{56}\text{Ca} - 2e^- + 2\nu_e$	0.1	0.01
$2.5 \cdot 10^{10}$	$^{56}\text{Ca} \Rightarrow ^{56}\text{Ar} - 2e^- + 2\nu_e$	0.11	0.01
$3.1 \cdot 10^{10}$	$^{56}\text{Ar} \Rightarrow ^{52}\text{S} + 4n - 2e^- + 2\nu_e$	0.12	0.01

Non-Equilibrium Processes in the Inner Crust

ρ (g cm^{-3})	Reaction	X_n	Q (Mev/np)
$9.1 \cdot 10^{11}$	$^{52}\text{S} \Rightarrow ^{46}\text{Si} + 6n - 2e^- + 2\nu_e$	0.07	0.09
$1.1 \cdot 10^{12}$	$^{46}\text{Si} \Rightarrow ^{40}\text{Mg} + 6n - 2e^- + 2\nu_e$	0.07	0.09
$1.5 \cdot 10^{12}$	$^{40}\text{Mg} \Rightarrow ^{34}\text{Ne} + 6n - 2e^- + 2\nu_e$		
	$^{34}\text{Ne} + ^{34}\text{Ne} \Rightarrow ^{68}\text{Ca}$	0.29	0.47
$1.8 \cdot 10^{12}$	$^{68}\text{Ca} \Rightarrow ^{62}\text{Ar} + 6n - 2e^- + 2\nu_e$	0.39	0.05
$2.1 \cdot 10^{12}$	$^{62}\text{Ar} \Rightarrow ^{56}\text{S} + 6n - 2e^- + 2\nu_e$	0.45	0.05
$2.6 \cdot 10^{12}$	$^{56}\text{S} \Rightarrow ^{50}\text{Si} + 6n - 2e^- + 2\nu_e$	0.5	0.06
$3.3 \cdot 10^{12}$	$^{50}\text{Si} \Rightarrow ^{44}\text{Mg} + 6n - 2e^- + 2\nu_e$	0.55	0.07
$4.4 \cdot 10^{12}$	$^{44}\text{Mg} \Rightarrow ^{36}\text{Ne} + 6n - 2e^- + 2\nu_e$		
	$^{36}\text{Ne} + ^{36}\text{Ne} \Rightarrow ^{72}\text{Ca}$		
$5.8 \cdot 10^{12}$	$^{68}\text{Ca} \Rightarrow ^{62}\text{Ar} + 6n - 2e^- + 2\nu_e$	0.61	0.28
$7.0 \cdot 10^{12}$	$^{62}\text{Ar} \Rightarrow ^{60}\text{S} + 6n - 2e^- + 2\nu_e$	0.7	0.02
$7.0 \cdot 10^{12}$	$^{60}\text{S} \Rightarrow ^{54}\text{Si} + 6n - 2e^- + 2\nu_e$	0.73	0.02
$9.0 \cdot 10^{12}$	$^{54}\text{Si} \Rightarrow ^{48}\text{Mg} + 6n - 2e^- + 2\nu_e$	0.76	0.03
$1.1 \cdot 10^{13}$	$^{48}\text{Mg} + ^{48}\text{Mg} \Rightarrow ^{96}\text{Cr}$	0.79	0.41
$1.1 \cdot 10^{13}$	$^{96}\text{Cr} \Rightarrow ^{88}\text{Ti} + 8n - 2e^- + 2\nu_e$	0.8	0.01

Deep Crustal Heating

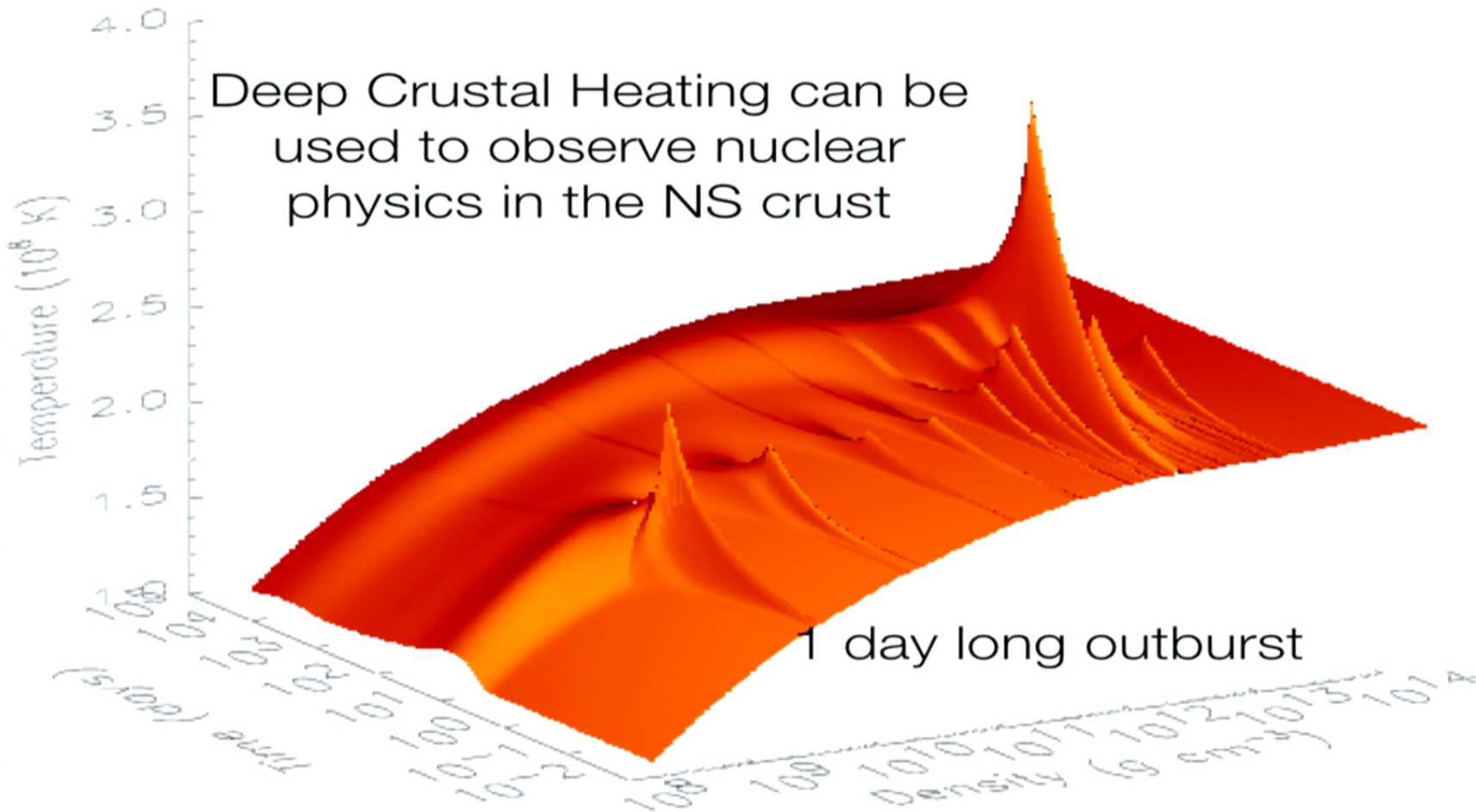
Begins Here
 Ends Here



1.47 Mev per np

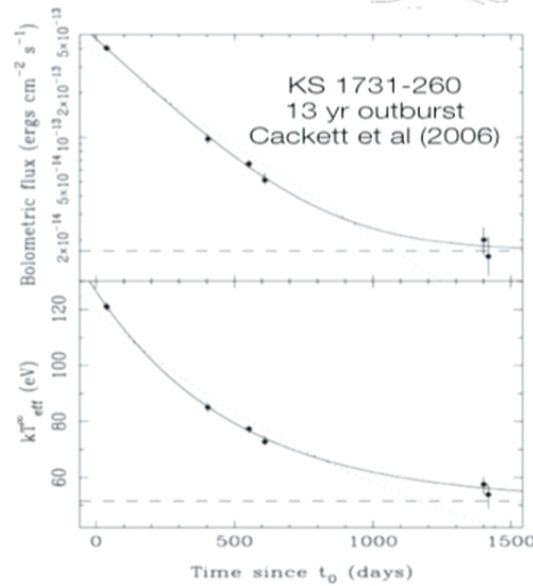
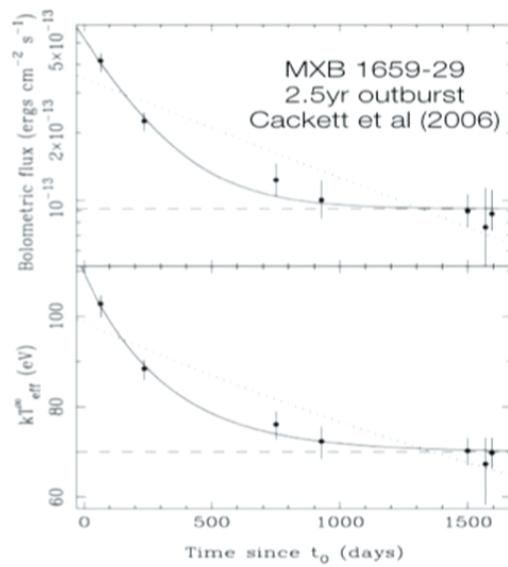
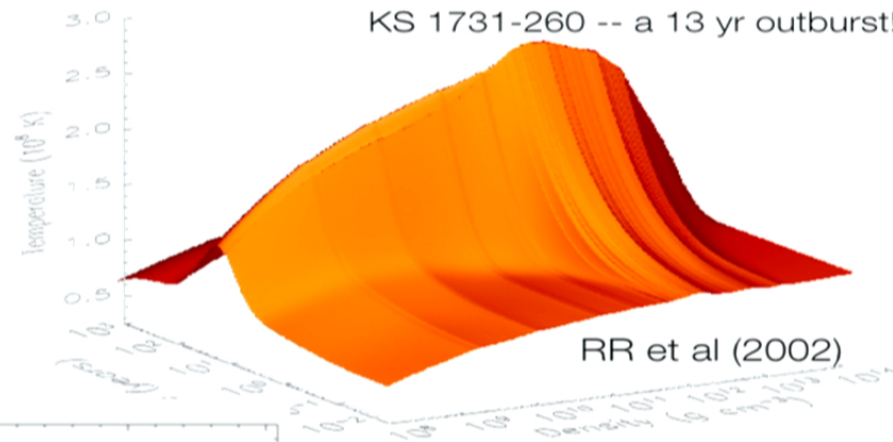
Brown, Bildsten & RR (1998)

Deep Crustal Heating can be used to observe nuclear physics in the NS crust



Ushomirsky & RR (2001)

Transient Neutron Star Cooling KS 1731-260 & MXB 1659-29



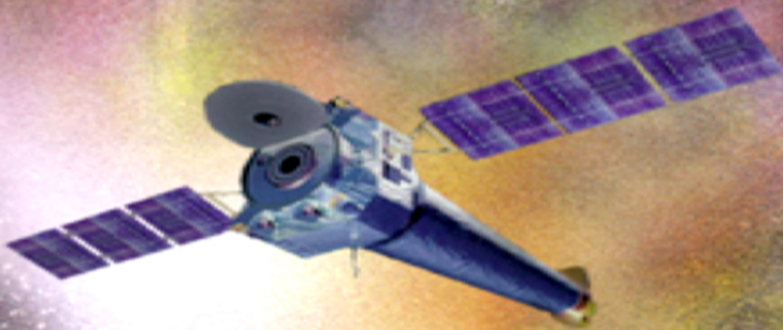
Sudden drop x3 in 2013? Cackett et al 2013

- Supports the Deep Crustal heating model.
- Permits exploring the nuclear physics of the crust.

Instruments for measurements of qLMXBs

Chandra X-ray Observatory

- Launched 1999 (NASA)
- 1" resolution



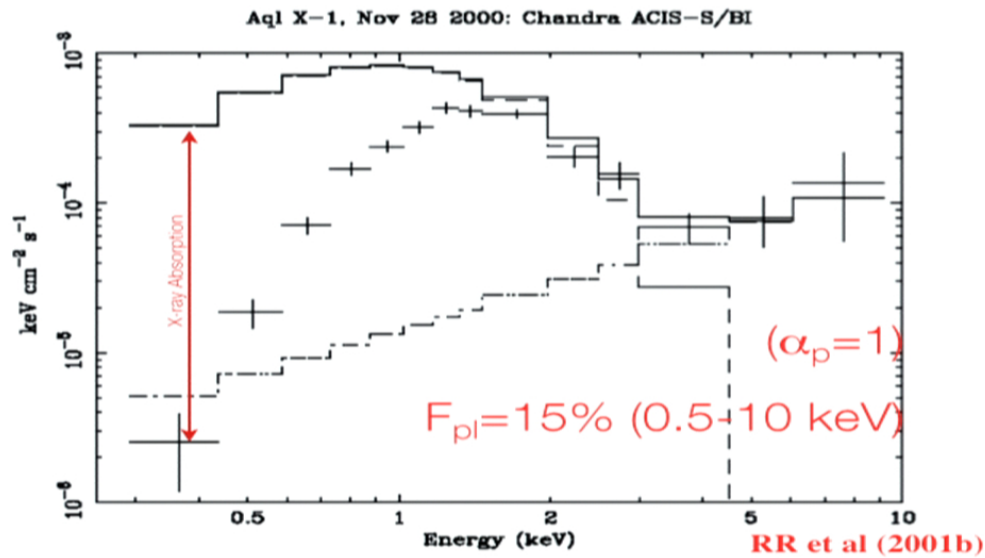
XMM/Newton

- Launched 1999 (ESA)
- 6" resolution
- ~4x area of Chandra.



Every photon is time tagged (~ 1 sec), with its energy measured ($E/\Delta E = 10$) with full resolution imaging.

Aql X-1 with Chandra -- Field Source



R_{∞} (d/5 kpc)

13_{-4}^{+5} km

$kT_{\text{eff},\infty}$

135_{-12}^{+18} eV

N_{H}

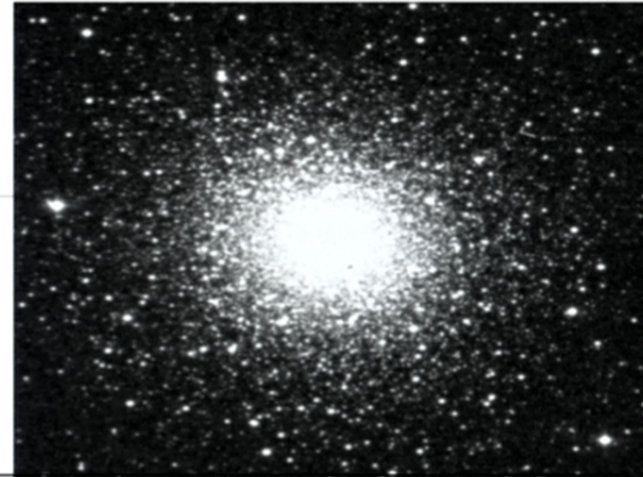
($1e20 \text{ cm}^{-2}$)

35_{-7}^{+8}

The LMXB Factories: Globular Clusters

- GCs : overproduce LMXBs by 1000x vs. field stars
- Many have accurate distances measured.

qLMXBs can be identified by their soft X-ray spectra, and confirmed with optical counterparts.



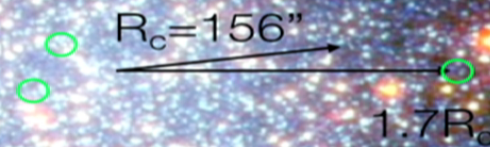
NGC	D (kpc)	+/- (%)
104	5.13	4
288	9.77	3
362	10	3
4590	11.22	3
5904	8.28	3
7099	9.46	2
6025	7.73	2
6341	8.79	3
6752	4.61	2

Carretta et al (2000)

NGC 5139 (Omega Cen)

qLMXBs can be identified by their soft X-ray spectra, and confirmed with optical counterparts.

The identified optical counterpart demonstrates unequivocally the X-ray source is a qLMXB.

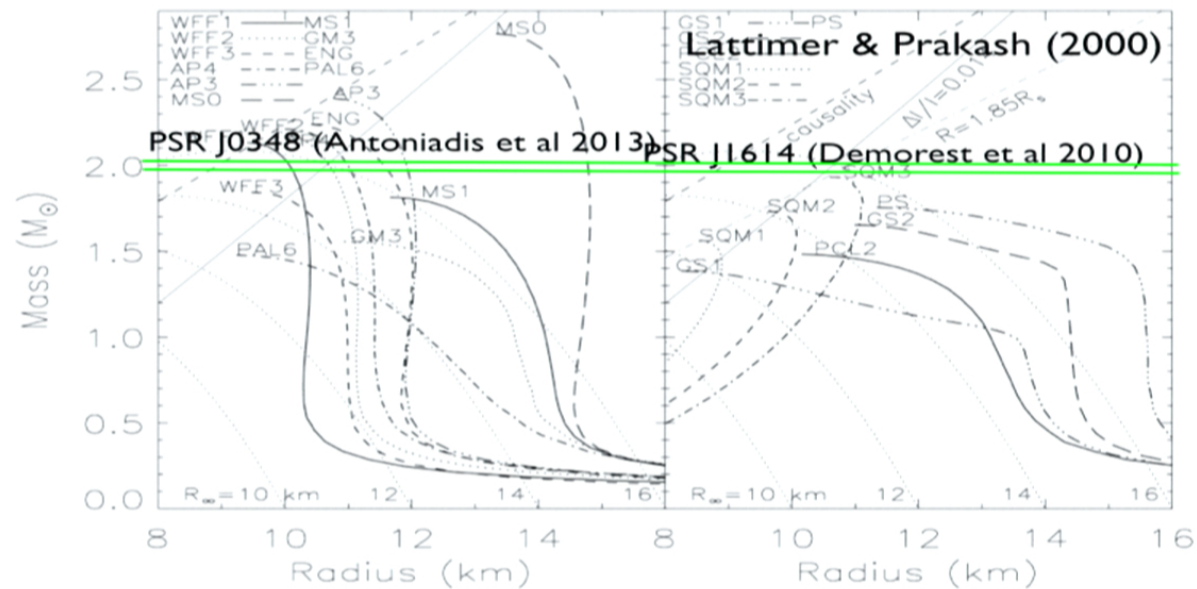


An X-ray source well outside the cluster core
Spitzer (Infrared)

Mass-Radius Relation from the Equation of State

Measuring the Mass and Radius simultaneously is difficult.

High-mass measurements prefer EOSs which produce a nearly constant radius at astrophysically interesting masses.



Precision Radius Measurements (<5%) may be the key to measuring the dEOS.

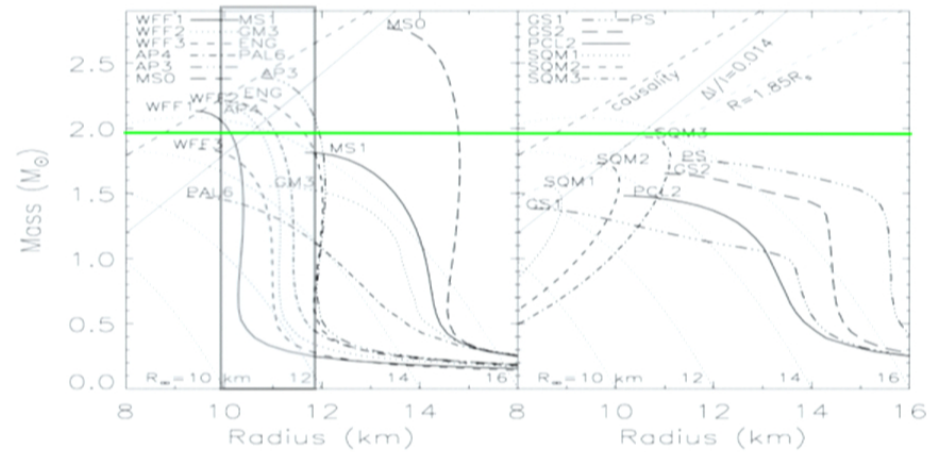
All qLMXBs used in this work were previously identified and analysed, with resulting R published.

Name	kT_eff(infty) (ev)	NH	Fx (10^{-13} cgsflux)	Band (keV)	Ref.	R(infty)
47 Tuc X7	105(5)	0.04(2)	5.3	0.5-10	Heinke et al (2006)	<: 5"
47 Tuc X5	100(20)	0.09(7)	4.3	0.5-10	Heinke et al (2003)	< 5"
M28	90(+30-10)	0.26(4)	3.4	0.5-8	Becker et al (2003)	<5"
NGC 6304 X9	115(20)	[0.266]	1.5	0.5-10	Guillot et al (2009)	+++
NGC 6304 X4	120(20)	[0.266]	1.1	0.5-10	Guillot et al (2009)	<15"
NGC 6397 (U24)	74(18)	0.1-0.26	1.06	0.5-2.5	Grindlay et al (2001)	< 15"
M13	76(3)	[0.011]	1.03	0.1-5	Gendre et al (2003)	DONE
NGC 3201 X16	170 (50)	[0.14]	1	0.6-6	Webb et al (2006)	Data taken
NGC 6553 X9	100 (20)	[0.35]	1	0.5-10	Guillot et al (in prep)	+++
Omega Cen	67(2)	0.09(3)	0.95	0.1-5	Rutledge et al (2002), Gendre et al (2003)	DONE
NGC 6637 X3	100 (40)	[0.11]	0.84	0.5-10	Guillot et al (in prep)	+++
M30 A-1	94(15)	0.03(1)	0.73	0.5-10	Lugger (2007)	<10"
NGC 6553 X3	127(+7-45)	[0.35]	0.65	0.5-10	Guillot et al (in prep)	<: 5"
NGC 6304 X5	70(25)	[0.266]	0.32	0.5-10	Guillot et al (2008)	+++
NGC 6553 x35	88 (60)	[0.35]	0.3	0.5-10	Guillot et al (in prep)	+++
NGC 2808 C2	--	0.86	0.24	--	Servillat et al (2008)	<15"
M80 CX2	82(2)	0.09(2)	0.23	0.5-6	Heinke et al (2003)	<5"
M80 CX6	76(6)	0.22(7)	0.07	0.5-6	Heinke et al (2003)	<15"

Measuring the Radius of Neutron Stars from qLMXBs in Globular Clusters

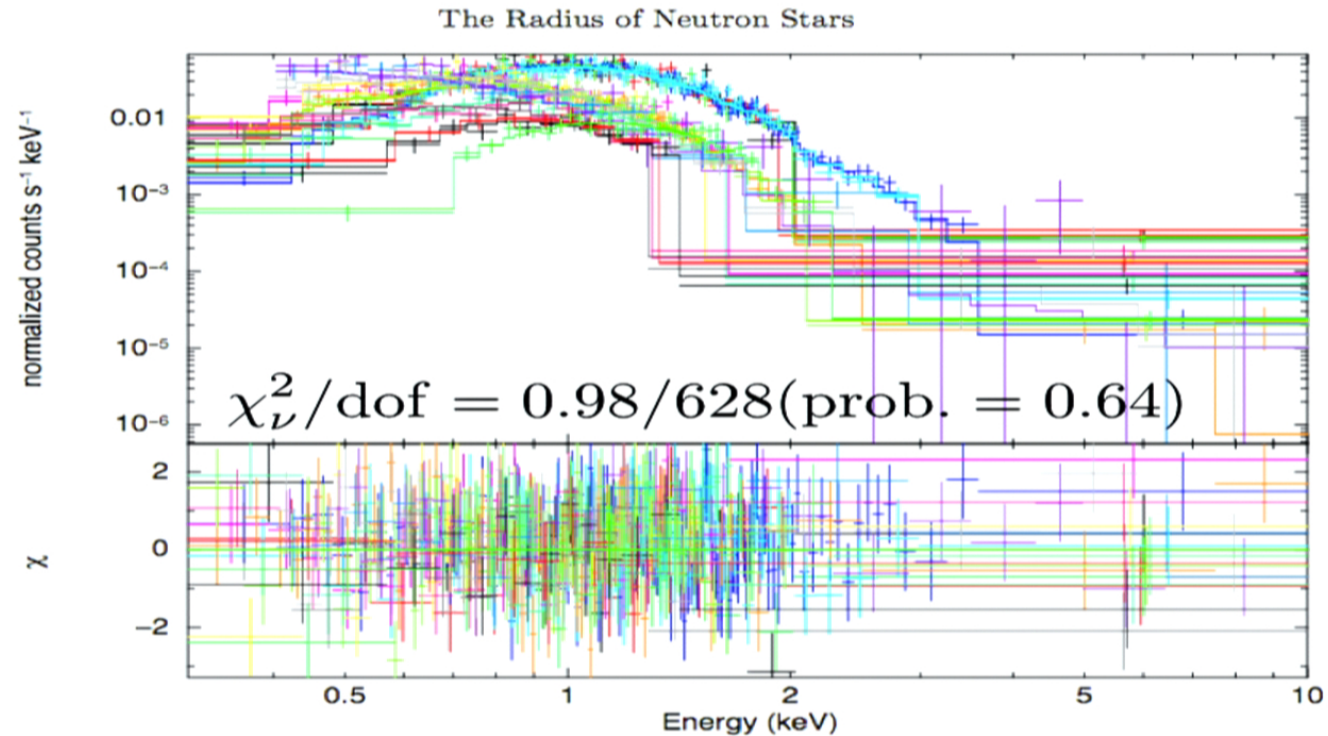


- The 2.0 solar mass neutron stars favor hadronic dEOSs over quark and phase-transition dEOSs. **These have the property of a quasi-constant neutron star radius.**
- Analysis goal: **Using all suitable qLMXB X-ray data sets of targets (there are five) provide the most reliable neutron star radius measurement possible.**
- Assume the radius of neutron stars is **quasi-constant** (a constant, at astrophysically important masses, within measurement error).
- Perform a Markoff-Chain-Monte-Carlo (MCMC) and include all known uncertainties and use conservative assumptions.



Best H atmosphere (+ PL) spectral fit of all 5 qLMXBs

- This model is a statistically acceptable fit to the X-ray spectral data. This is an a posteriori confirmation that the data are consistent with our assumptions.
- After finding the best fit a MCMC method was used to find the uncertainty regions for all parameters - -- the Radius, Mass, Temperature, absorption, distance, and power-law normalization.



Guillot et al (2013)

NH free, D gaussian bayesian priors, PL included.

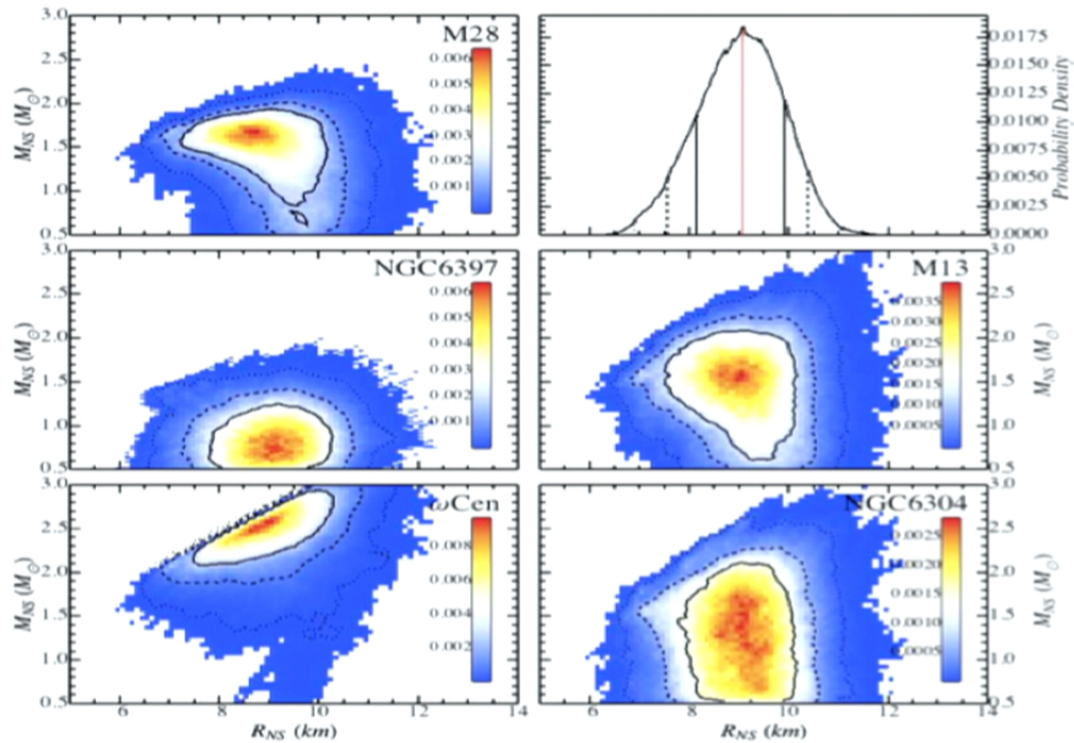
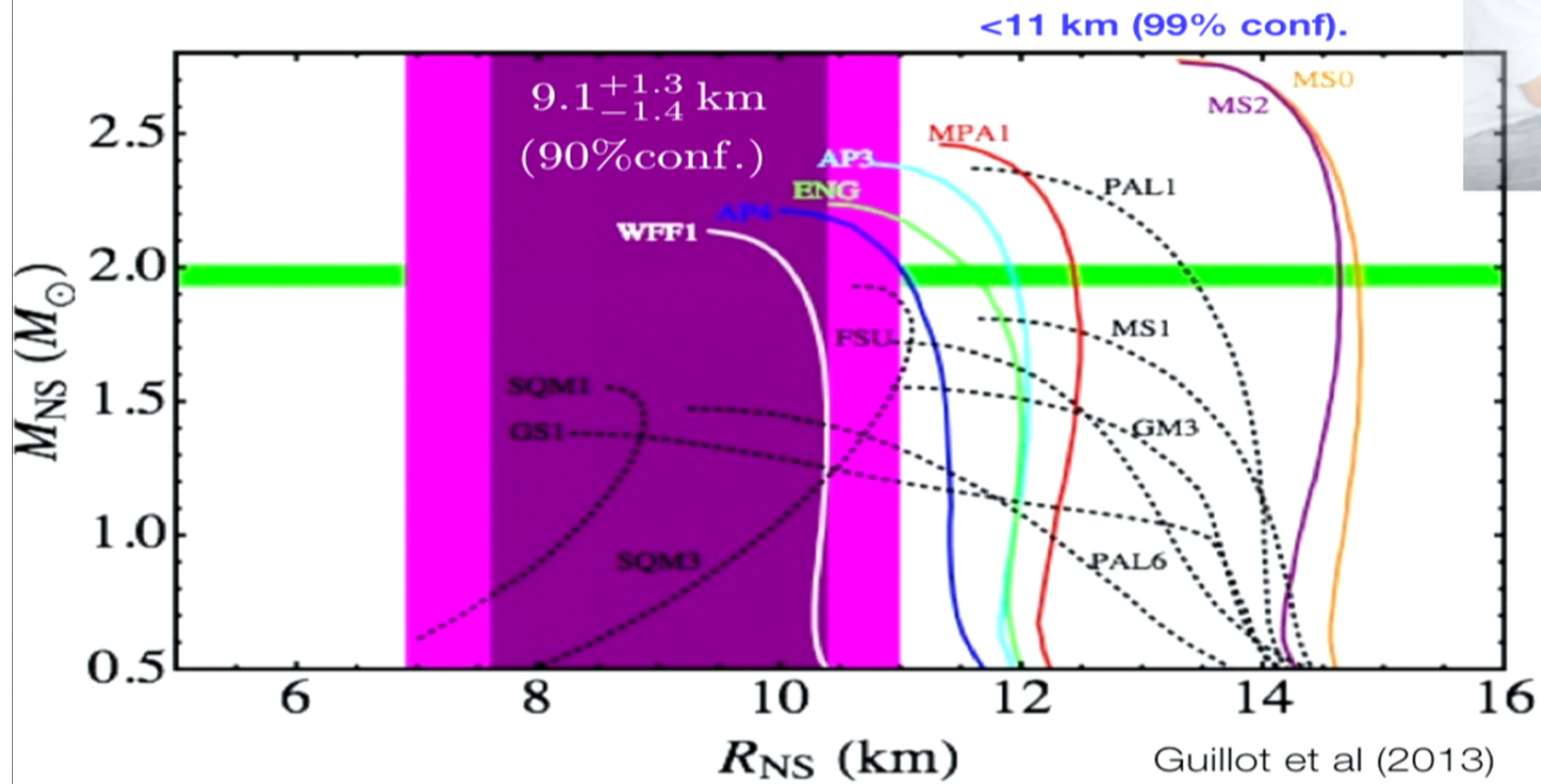


FIG. 15.— Figure similar to Figure 9 corresponding to Run #7. Here, all the possible assumptions have been relaxed to obtain a R_{NS} measurement the least affected by systematic uncertainties. The N_H parameters are left free; and Gaussian Bayesian priors and PL components are included. This results in an R_{NS} measurement: $R_{NS} = 9.1^{+1.3}_{-1.2}$ km

Guillot et al (2013)

The Neutron Star Radius



M-R by J. Lattimer

WFF1 = Wiring, Fiks and Fabrocini (1988)

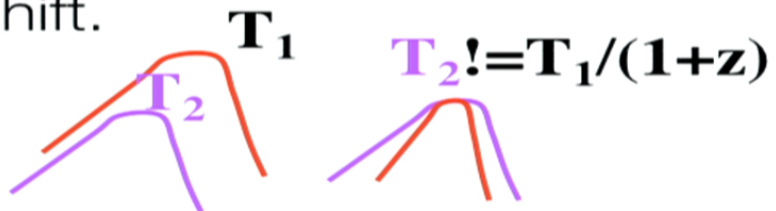
Contains uncertainties from:
Distance
All spectral parameters
Calibration

Mass Measurements with Continuum Spectra

You cannot measure a redshift from blackbody emission due to photon energy (E) temperature (kT) degeneracy.

$$I(E_\gamma) \propto \left(\frac{E_\gamma}{kT}\right)^3 \frac{1}{e^{\frac{E_\gamma}{kT}} - 1}$$


- But, the free-free opacity breaks this degeneracy. This spectrum, redshifted, permits (in principle) determination of the redshift.

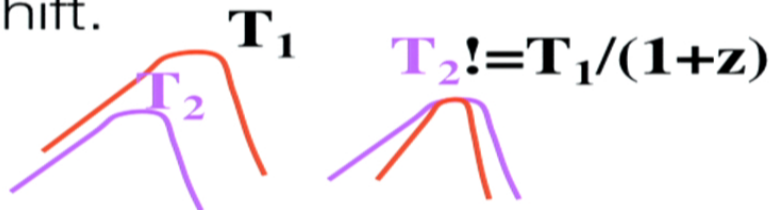
$$I(E_\gamma) \propto \left(\frac{E_\gamma}{kT}\right)^3 \frac{1}{e^{\frac{E_\gamma}{kT}} - 1} \kappa_{ff,o} \left(\frac{E_o}{E_\gamma}\right)^3$$


Mass Measurements with Continuum Spectra

You cannot measure a redshift from blackbody emission due to photon energy (E) temperature (kT) degeneracy.

$$I(E_\gamma) \propto \left(\frac{E_\gamma}{kT}\right)^3 \frac{1}{e^{\frac{E_\gamma}{kT}} - 1}$$


- But, the free-free opacity breaks this degeneracy. This spectrum, redshifted, permits (in principle) determination of the redshift.

$$I(E_\gamma) \propto \left(\frac{E_\gamma}{kT}\right)^3 \frac{1}{e^{\frac{E_\gamma}{kT}} - 1} \kappa_{ff,o} \left(\frac{E_o}{E_\gamma}\right)^3$$


Mass Measurements
with Continuum Spectra

$$R_\infty \rightarrow$$

$$T_\infty \rightarrow$$

Normalization

Peak of the spectrum

$$z = \frac{GM_{NS}}{c^2 R_{NS}} \rightarrow \text{Second Derivative at the Peak of the Spectrum}$$

$$I(E_\gamma) \propto \left(\frac{E_\gamma}{kT}\right)^3 \frac{1}{e^{\frac{E_\gamma}{kT}} - 1}$$



- But, the free-free opacity breaks this degeneracy. This spectrum, redshifted, permits (in principle) determination of the redshift.

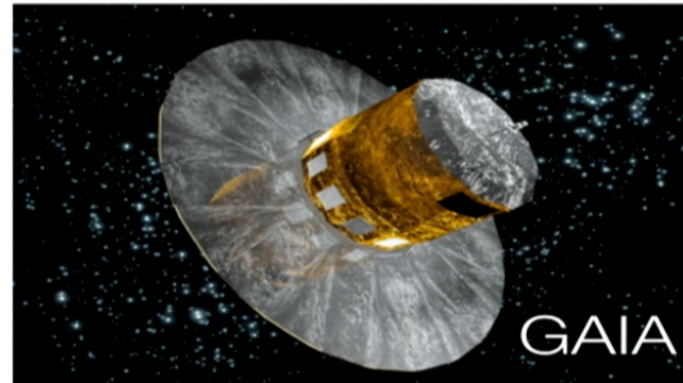
$$I(E_\gamma) \propto \left(\frac{E_\gamma}{kT}\right)^3 \frac{1}{e^{\frac{E_\gamma}{kT}} - 1} \kappa_{ff,o} \left(\frac{E_o}{E_\gamma}\right)^3$$



Measuring Distances: GAIA Mission Capabilities

- An European Space Agency Cornerstone Mission, now operating at L2.

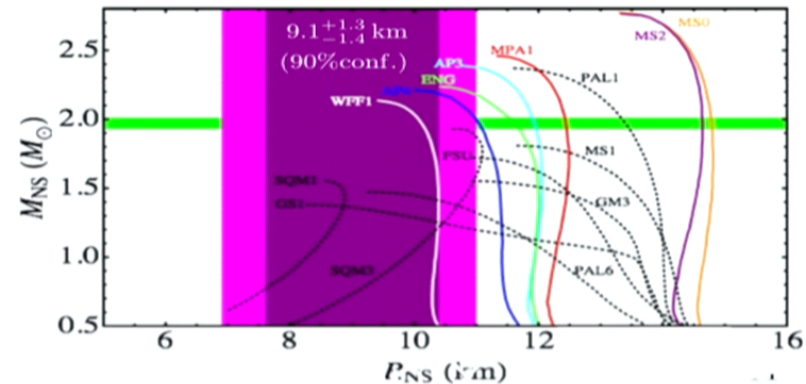
V	# (millions)	σ_{μ} -arcsec	3% Distance (kpc)
10	0.34	7	4.2
15	26	22	1.4
20	1000	250	0.12



Are there enough qLMXBs within this distance?

Simultaneous Mass and Radius Measurements of Neutron Stars

- We have measured the neutron star radius, to 15% accuracy, in a model dependent way.
- Significant work remains to confirm many of the assumptions behind this approach.
- With a mere handful of simultaneous mass-radius measurements -- 5-7 -- this will measure a specific dense matter equation of state. This is do-able with the next generation X-ray calorimeters which will begin to be launched in 2018 (Astro-H).



Assumptions -- the systematic uncertainties.

- **H atmosphere neutron stars.** Expected from a Hydrogen companion LMXB; can be supported through optical observations of a H companion.
- **Low B-field ($<10^{10}$ G) neutron stars.** This is true for 'standard' LMXBs as a class, but difficult to prove on a case-by-case basis.
- **Emitting isotropically.** Occurs naturally when powered by a hot core.
- **Non-Rotating neutron stars.** qLMXBs are observed to rotate at 100-600 Hz. This can be a significant fraction of the speed of light. Doppler boosting and deviation from NS spheroidal geometry are not included in emission models. *These effects should be calculated, but have not yet been.*

If you don't like these assumptions: "We find the assumptions not strongly supported and therefore ignore this result."

The Dense Matter Equation of State is an important Strong Force Regime

Each different proposed dEOS produces a different mass-radius relationship for neutron stars.

Thus, measure the mass-radius relationship of neutron stars, and you have a measurement of the dEOS.

Precision requirement -- 5% in mass and radius, separately.

A larger uncertainty is useless to nuclear physics.

